Paper No. PIIB.3

THE 13TH INTERNATIONAL STELLARATOR WORKSHOP

QPS CONFINEMENT AND TRANSPORT

Spong[1], D.A., Berry[1], L.A., Hirshman[1], S.P., Lyon[1], J.F., Mikkelsen[2], D.

[1] *Oak Ridge National Laboratory, P.O. Box 2009, Oak Ridge, TN 37831-8073*

[2] *Princeton Plasma Physics Laboratory, P.O. Box 451, Princeton, NJ 08502*

Abstract. Quasi-poloidal symmetry is a new approach to stellarator confinement optimization that we have used to design very low plasma aspect ratio configurations (<R>/<a>≈1.6, 1/2–1/4 that of existing stellarators). An experiment, the Quasi-Poloidal Stellarator (QPS), is being developed to test the main features of this approach. QPS has <R> = 0.9 m, <a>≈ 0.35 m, $\langle B_0 \rangle \approx$ 1 T for a 0.5-s pulse, and $P_{heating}$ = 1-3 MW. An important criterion for our optimization has been to achieve sufficiently low levels of neoclassical transport so that the dominant losses are from anomalous transport. A number of recently developed/improved tools have been used to evaluate both perpendicular and parallel transport properties (bootstrap current, neoclassical resistivity enhancement) in this device. These include: the DKES transport coefficient code, the DELTA5D Monte Carlo model, and several 0-D and 1-D models. We will apply these models to the QPS configuration and discuss the neoclassical properties of the various transport regimes it can access.

I. Introduction

The design of low aspect ratio stellarators has been guided by the goal of maintaining adequate levels of neoclassical and energetic particle confinement. The compact geometries of these devices inherently couple together strong toroidal/poloidal/helical shape variations. Transport properties, however, depend on the symmetries of the magnetic field in Boozer coordinates[1]. Sufficient symmetries in these particular coordinates can be achieved at low aspect ratio through a process of numerical optimization.

In this paper we analyze the transport properties of low aspect ratio devices with quasi-poloidal symmetry. For this form of symmetry, the dominant components of the magnetic field have the poloidal mode number m equal to zero. In the limit of exact poloidal symmetry, the canonical poloidal angular momentum P_θ would be conserved and the orbit excursions away from a flux surface would be limited by the gyroradius in the toroidal magnetic field ρ_{tor} rather than the gyroradius in the poloidal magnetic field ρ_{pol} (banana width) as is the case for axisymmetric devices. Since $\rho_{tor} \ll \rho_{pol}$, this can lead to substantial reductions in neoclassical transport. Another way of viewing this is to consider that of the three possible forms of stellarator symmetry, poloidal symmetry (for low rotational transform devices) most nearly aligns the direction of $\vec{B}$ and $\vec{\nabla}|B|$, thus minimizing cross field drifts. Further properties of devices with exact poloidal symmetry would be minimal flow damping in the poloidal direction and reduction of the bootstrap current by a factor of ι/N_{fp} where ι is the rotational transform (=1/q) and N_{fp} is the number of field periods. Of course, exact poloidal symmetry has not been achieved in realizable devices and, for this reason, transport analysis of these configurations (taking into account multi-helicity effects) is an important issue. Our design goal has been to reduce neoclassical transport to levels sufficiently below

the expected anomalous transport[2] so that noticeable transport reduction would be observed if enhanced confinement regimes are accessible.

In Figure 1 two views of the outer magnetic flux are shown for our current reference QPS configuration. The poloidally symmetric structure is evident at least for the side sections by the banded structure of the magnetic field strength contours. The degree to which the end sections can be made poloidally symmetric is somewhat related to how thin (elongated) they can be made. For the design of the QPS device (<R> = 0.9 m, <a>≅ 0.35 m, $\langle B_0 \rangle \cong 1$ T) the minimum thickness of the plasma in these regions has been limited to ~20-25 cm, motivated by a desire to minimize neutral penetration. In larger devices, such a constraint will be less limiting with respect to allowable elongations in the end regions.

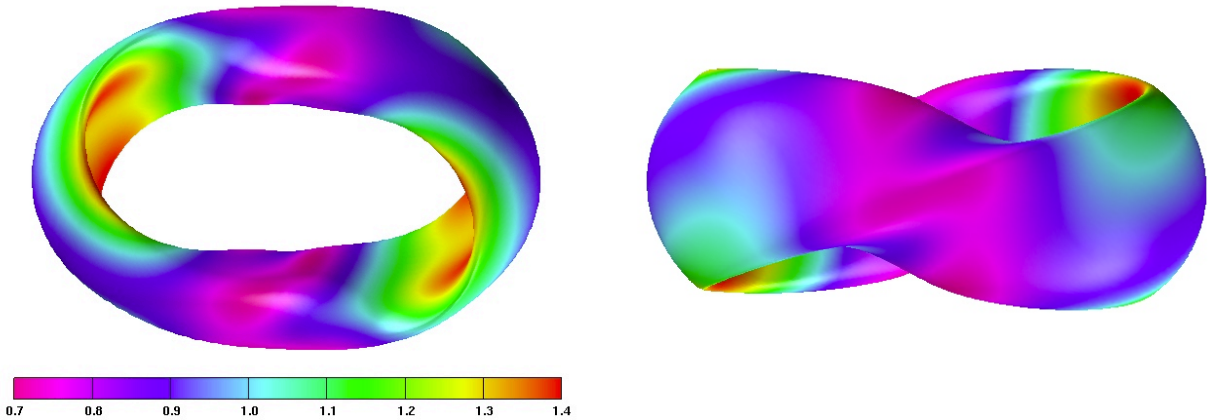

Figure 1 – Top and side views of the outer flux surface of the QPS device with color coding used to indicate the magnetic field strength (in Tesla).

The outer flux surfaces shown in Figure 1 are generally the location where the largest deviations from poloidal symmetry occur. However, since transport in edge regions will likely be dominated by fluctuations, impurities, neutrals, etc., the more important measures of poloidal symmetry are from the inner flux surfaces. In Figure 2 the magnetic field strength contours are plotted for a surface at $\sqrt{\Box/\Box_{max}} = 0.3$ and show the strong poloidal symmetry particularly for the magnetic well regions (B < 1 Tesla) shown in blue.

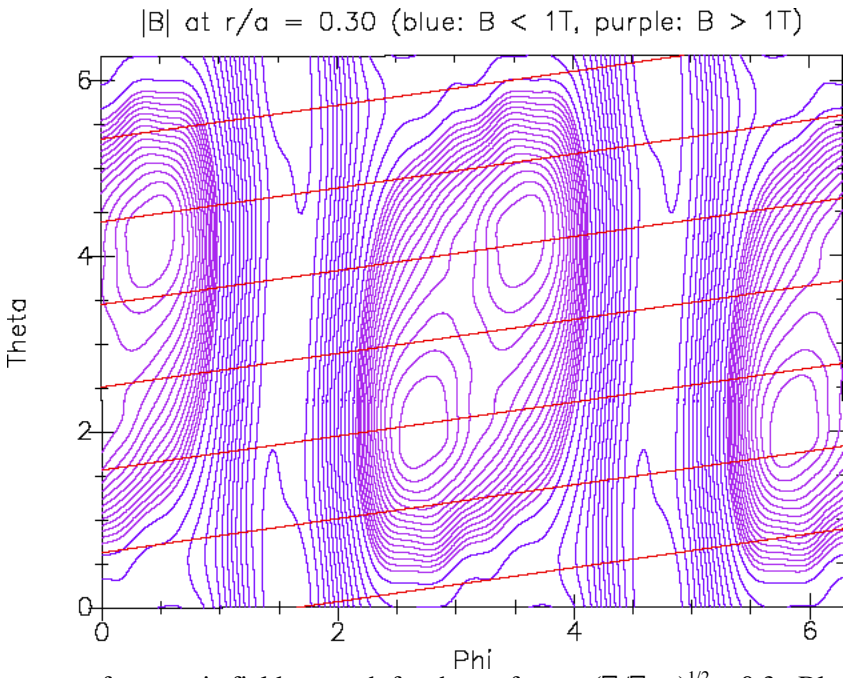

Figure 2 – Contours of magnetic field strength for the surface at $(\Phi/\Phi_{max})^{1/2} = 0.3$. Blue contours are for B < 1 Tesla while purple contours are for B > 1 Tesla. Magnetic field lines are indicated in red.

In Figure 3 the larger Fourier components of |B| are plotted against normalized flux labeled with their respective poloidal and toroidal mode numbers (m,n). As may be seen, near the axis, the poloidally symmetric (m,n) = (0,1) and (0,2) modes dominate. Further out, the (1,0) and (1,1) modes enter in with the (1,0) mode being down about a factor of 2 over what it would be in the equivalent R_0/<a> axisymmetric device.

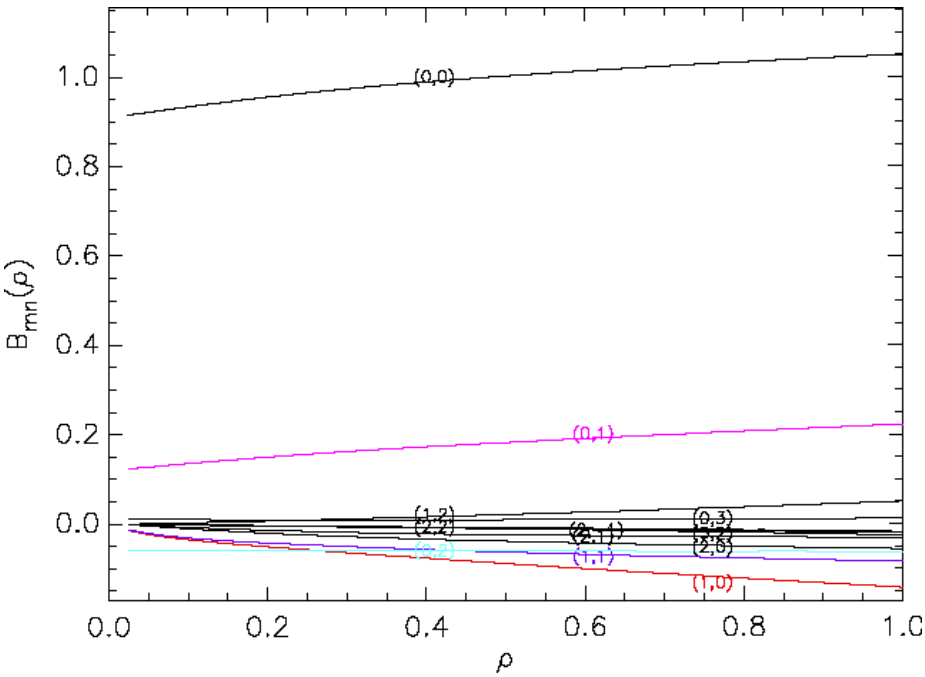

Figure 3 – Fourier components of |B| vs. normalized flux and (m,n) number.

One further measure of quasi-poloidal symmetry is shown in Figure 4. This is the ratio of the magnetic energy in the modes without poloidal symmetry to those with poloidal symmetry (excluding m = 0, n = 0). This ratio reduces the multiple curves of Figure 3 to a single curve.

Figure 4 displays this measure for the current QPS configuration (labeled QPS-1108a4) along with some of its predecessors. As can be seen, significant progress has been made in improving the poloidal symmetry since our initial QPS configuration[3] of 2 years ago.

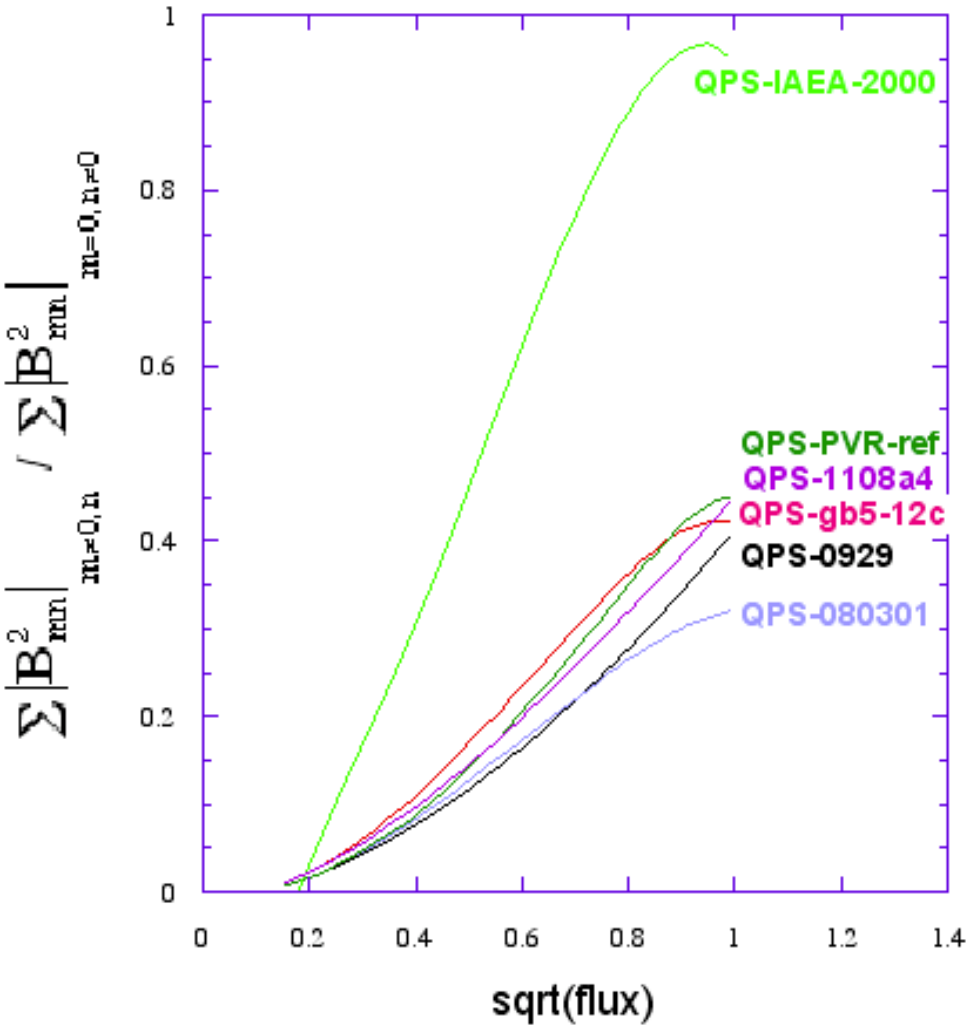

Figure 4 – Ratio of magnetic energy in non-poloidally symmetric modes to energy in poloidally symmetric modes for different QPS configurations vs. $(\Box/\Box_{max})^{1/2}$.

The results shown in Figures 1 through 4 have been based on QPS devices with <□>'s in the 1.8□ 2% range and with rotational transform profiles rising toward the plasma edge, as is characteristic of stellarators. These devices generally have second stability regimes for <□>'s in the 7 – 15% range. High <□> has desirable effects on quasi-poloidal symmetry and energetic particle confinement. A closely related set of QPS configurations[4] is under development with rotational transform profiles that decrease towards the plasma edge and which have good access to second stability. A typical B_{mn} spectrum for one of these devices at <□> = 15% is shown in Figure 5. As can be seen, the non-poloidally symmetric modes are even further suppressed here than in Figure 3. Also, there is a more significant radial variation in the $B_{0,0}$ component (due to the finite <□> diamagnetic suppression of the magnetic field). This gradient acts to improve the confinement of energetic trapped particles in a way (through increased poloidal drifts) that is analogous to how radial electric fields improve confinement for thermal trapped particles.

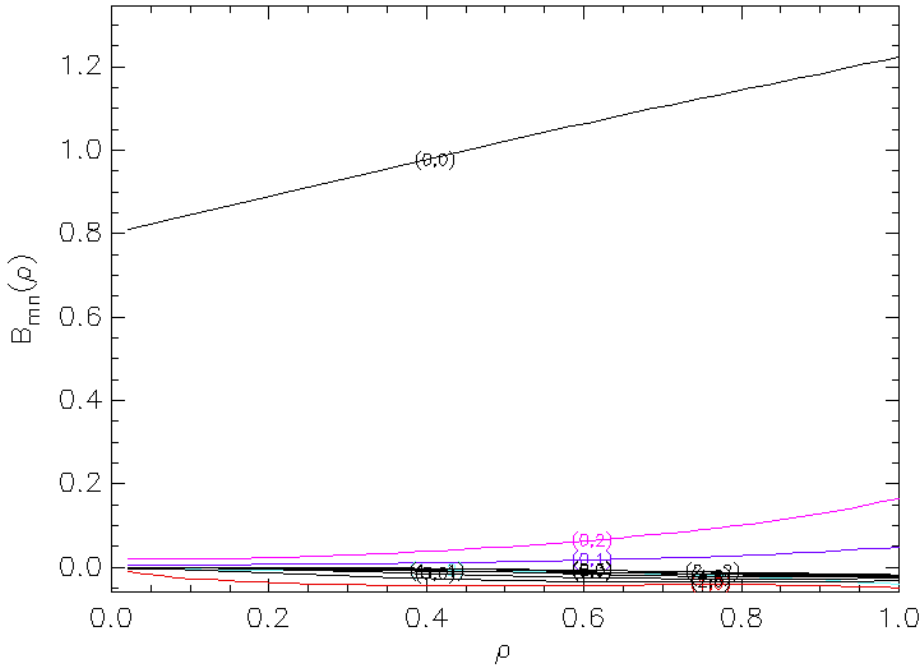

Figure 5 – Fourier components of |B| vs. normalized flux and (m,n) number for a <β> = 15% QPS configuration.

II. Local Transport Coefficient Evaluations

We have evaluated and compared the neoclassical confinement properties of QPS devices using several theoretical models based on local diffusive transport assumptions. The tools used have been the low collisionality NEO[5] code and the DKES model.[6] In Figure 6 we plot the low collsionality effective ripple coefficient $\epsilon_{eff}^{3/2}$ obtained from the NEO code for various QPS and torsatron configurations. As can be seen, reductions in this parameter have been achieved for more recent QPS configurations (1108) as compared to some of the earlier devices (the configurations with "free" at the end of the name are based on free boundary reconstructions). As will be discussed in the flexibility section, the vertical field can be used to shift the QPS magnetic axis inward. This leads to further reductions in $\epsilon_{eff}^{3/2}$ (especially near the center) as can be seen by comparing the QPS_1108_shifted_in and QPS_1108_free curves.

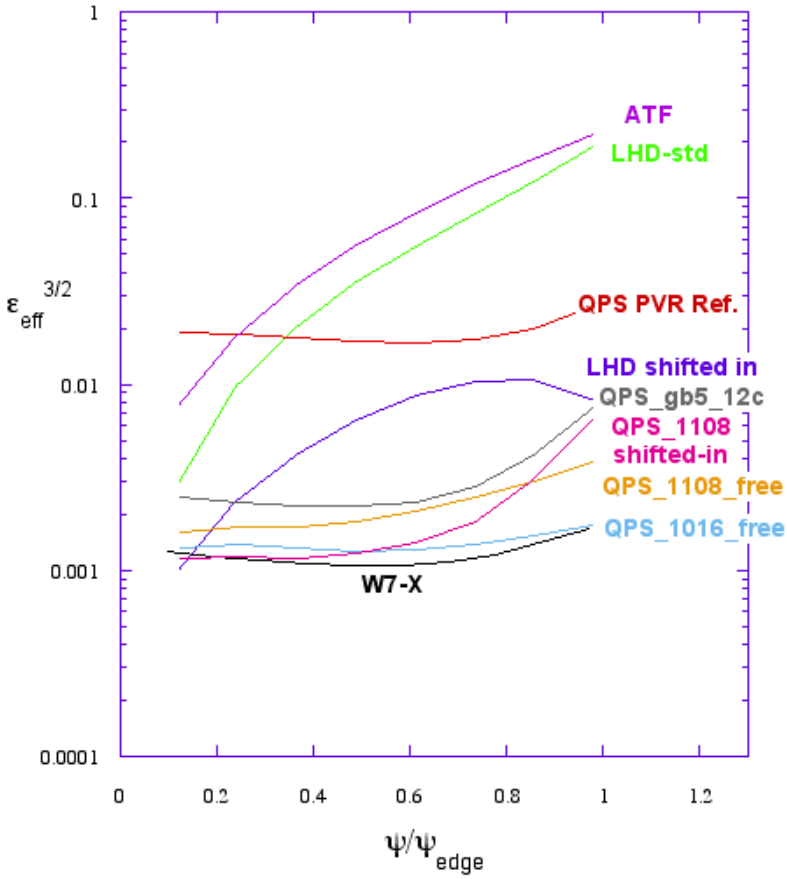

Figure 6 – Low collisionality effective ripple coefficient $\varepsilon_{eff}^{3/2}$ from the NEO[5] code for various QPS and torsatron configurations.

The drift kinetic solver DKES[Error! Bookmark not defined.] calculates the full stellarator neoclassical transport coefficient matrix for realistic magnetic field spectra of aribitrary helicity. This provides the coefficients needed to evaluate local heat and particle fluxes, self-consistent ambipolar electric fields, and bootstrap current levels. DKES has been applied to the reference configurations over the ranges of collisionality and electric field that provide reasonable convergence of the upper and lower bounds. Although a sufficient range of collisionalities and electric fields cannot be accessed to do the required energy integrations for all parameters of experimental interest, the monoenergetic coefficients provide useful physical insights over the parameter ranges where they can be converged. Also, a mixed model can be used where the DKES coefficients are employed over the ranges where they can be converged and then asymptotic forms are used to extrapolate outside these ranges. In Figure 7 we plot the DKES L_{11} coefficient for a flux surface about 1/2 of the way out (in flux) for an earlier QPS configuration (080301) as a function of collisionality and electric field. Also indicated by rectangular boxes are the approximate ranges of collisionality that are accessed in calculating the D_{22} thermal diffusivity coefficient for ECH and ICH heated regimes at B = 1 T. The ECH regime is n(0) = 1.8 x 10^{19} m^{-3}, $T_e(0)$ = 1.4 keV, and $T_i(0)$ = 0.15 keV; the ICH regime is n(0) = 8.3 x 10^{19} m^{-3}, $T_e(0)$ = 0.5 keV, and $T_i(0)$ = 0.5 keV. These ranges are estimated as the intervals in ν/v and E/v associated in going from thermal energies to 9 times thermal energies (for D_{22} the integrand has its maximum about halfway

through this range). These intervals are: ECH electrons ($7\times10^{-5} < \nu/v < 10^{-3}$, $8\times10^{-5} < E/v < 2\times10^{-4}$), ECH ions ($6\times10^{-3} < \nu/v < 7\times10^{-2}$, $10^{-2} < E/v < 3\times10^{-2}$), ICH electrons ($3\times10^{-3} < \nu/v < 4\times10^{-2}$, $5\times10^{-5} < E/v < 2\times10^{-4}$), ICH ions ($2\times10^{-3} < \nu/v < 3\times10^{-2}$, $2\times10^{-3} < E/v < 6\times10^{-3}$).

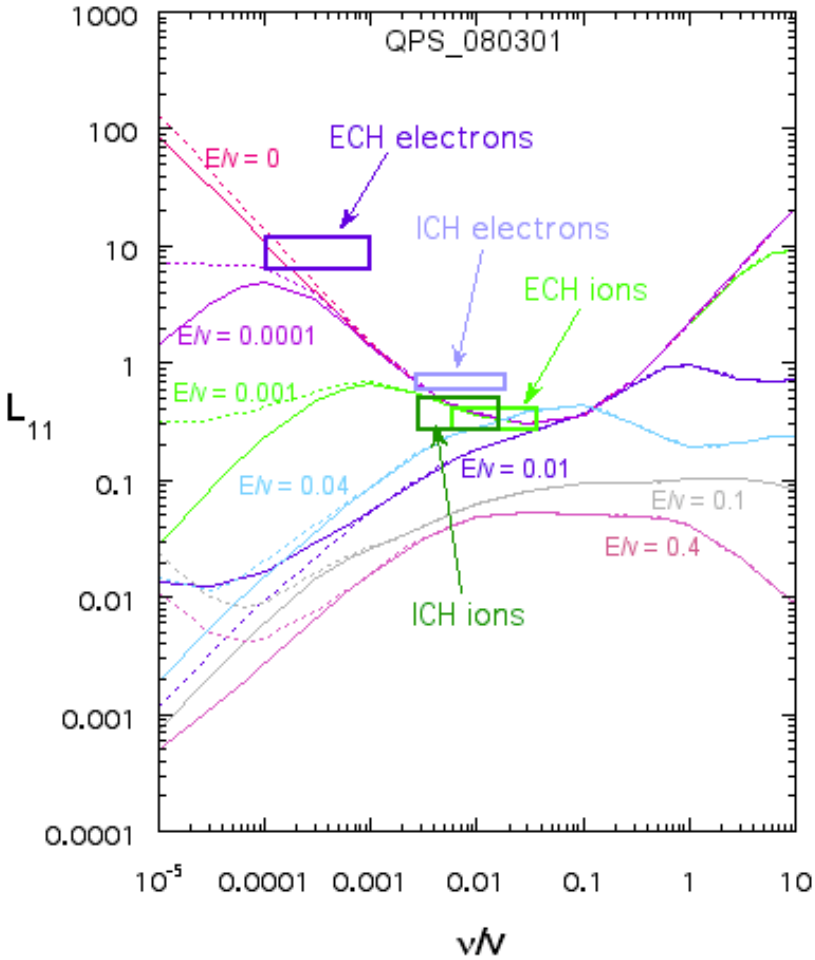

Figure 7 – Variation of DKES monoenergetic L_{11} transport coefficient with collisionality and electric field for a flux surface at $\psi/\psi_{max} = 0.5$. Parameter regimes for electrons and ions with ECH and ICH heating are indicated (the solid and dashed lines are the upper and lower bounds on L_{11} that DKES calculates).

As can be seen, the ECH electrons are well into the collisionless $1/\nu$ regime, while the ions and ICH electrons are more in the plateau regime.

The collisionality variation of the L_{11} transport coefficient has also been a useful measure of confinement when comparing different QPS configurations. In principle, at low collisionality, this can provide information equivalent to the NEO[5] calculation. The variation of the L_{11} transport coefficient with collisionality (taking $E_r = 0$) for various configurations is plotted in Figure 8. Here we have scaled each device to have the same major radius. As can be seen by comparing Figures 6 and 8, the DKES and NEO results do seem to show a similar ordering of transport levels between the different devices. Also, the ratio of L_{11}'s and $\varepsilon_{eff}^{3/2}$'s between the different devices is similar.

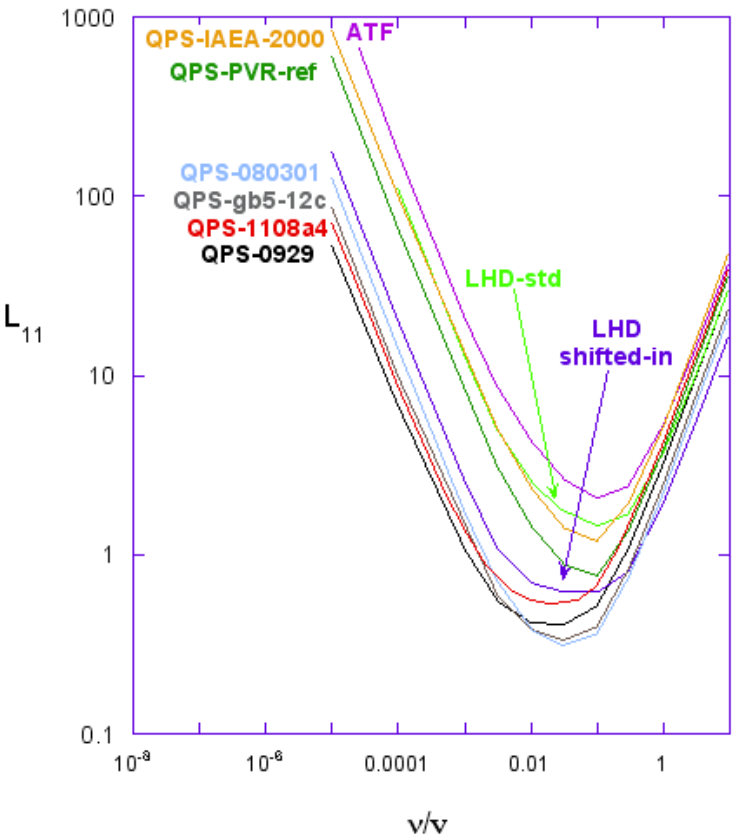

Figure 8 – Variation of DKES monoenergetic L_{11} transport coefficient with collisionality for a flux surface at $\square/\square_{max} = 0.5$ for several different QPS and torsatron configurations.

III. Monte Carlo simulations of QPS devices

Global Monte Carlo calculations based on the DELTA5D code[7] have also been used to compare various QPS configurations. Typically, full-f calculations are carried out and the complete guiding center orbits are followed; thus, both diffusive and direct orbit losses are included. An initial loading of particles is made over the cross-section of the device with the particle distributions determined by the density and temperature profiles. This ensemble of particles is then followed for a sufficient period of time so that the loss rate of particles through the outer surface reaches an approximate equilibrium. As particles leave the outer flux surface, they are re-seeded back into the plasma at random energies and locations consistent with the assumed profiles. In Figure 9 Monte Carlo ion energy confinement times are displayed for a range of configurations based on ICH [Figure 9(a)] and ECH [Figure 9(b)] heated parameters.

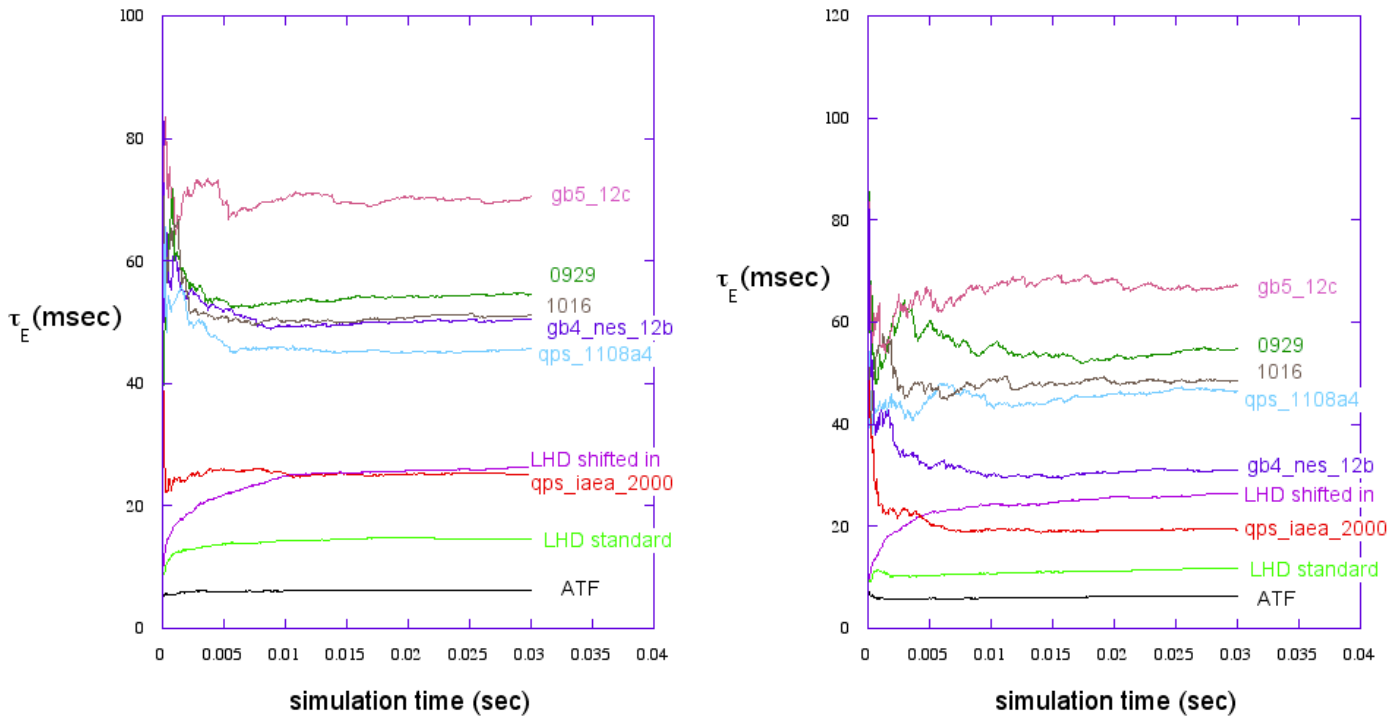

(a) (b)

Figure 9 – Monte Carlo global ion energy confinement times for ions in (a) ICH heated plasmas and (b) ECH heated plasmas (for densities and temperates of these cases, see section II.

These confinement times also show somewhat similar variations between devices as the DKES and NEO results had shown earlier; however, there are also some differences with the local transport orderings. This is likely due to the fact that these Monte Carlo results take into account the whole plasma volume and, as indicated in Figure 7, the ion ICH and ECH regimes are in the plateau collisionality regime whereas the NEO results are only applicable to lower collisionalities.

Monte Carlo calculations have also been used to assess electron confinement times in QPS devices, and to search for electric field values that give approximate ambipolar balances. These calculations have been documented elsewhere and will not be covered here.[7] Taking into account both ion and electron losses at expected values of the ambipolar electric field, we have found that neoclassical energy confinement times in the range of 2 – 7 times the ISS95 empirical scalings[2] are possible.

IV. QPS Flexibility Studies

QPS is being designed with 3 independently controllable sets of magnetic field coils: the modular field coils, the toroidal (i.e., B 1/R) field coils, and the vertical field coils. These coils are expected to provide a valuable source of flexibility for testing various QPS physics issues. Recently we have started to evaluate the effects of varying the currents in these different coilsets on neoclassical transport levels.

The vertical field generally shifts the plasma magnetic axis inward or outward and can influence the degree of magnetic field ripple and its symmetry properties. An example of this effect is shown in Figures 10(a) and 10(b). Here QPS magnetic field strength contours are

shown for a flux surface halfway out in radius for (a) a shifted-in case with I_{VF} = -30 kAmps, and (b) a shifted–out case with I_{VF} = 50 kAmps. The shifted-in contours are generally smoother and more quasi-poloidally symmetrical than the shifted-out contours.

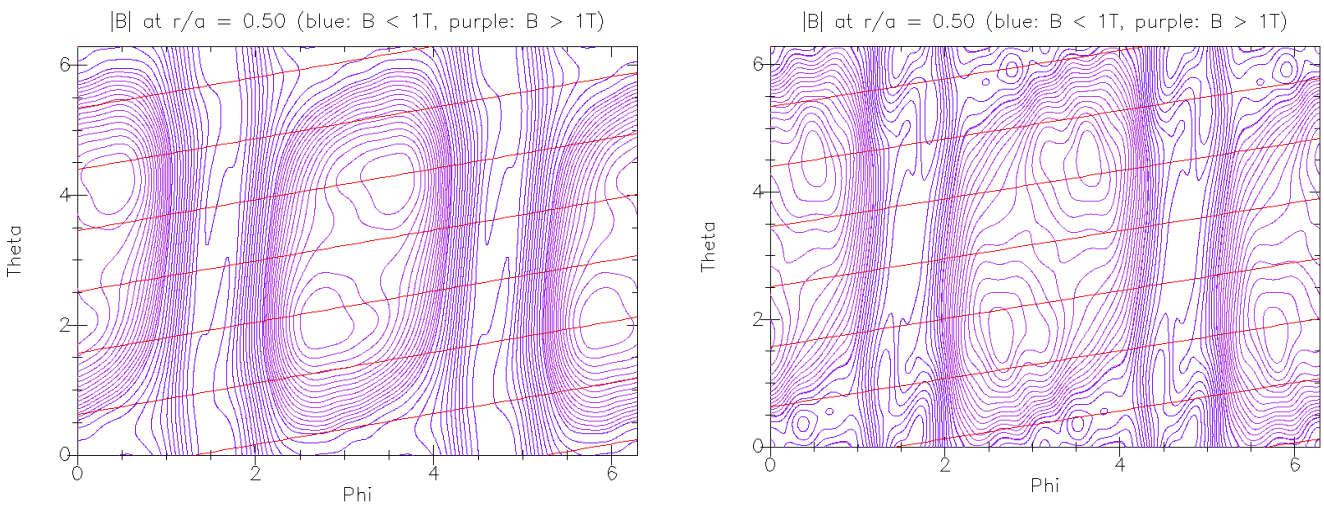

(a) (b)

Figure 10 – Magnetic field strength contours for a QPS plasma which is (a) shifted inward in major radius and (b) shifted outward in major radius.

The effect of the improved poloidal symmetry that results when the plasma is shifted inward is also reflected in Figure 11. Here the NEO code has been applied over a range of vertical field coil currents ranging from –30 kAmps to +50 kAmps and indicates that lower effective ripple levels are achieved for the shifted-in configurations.

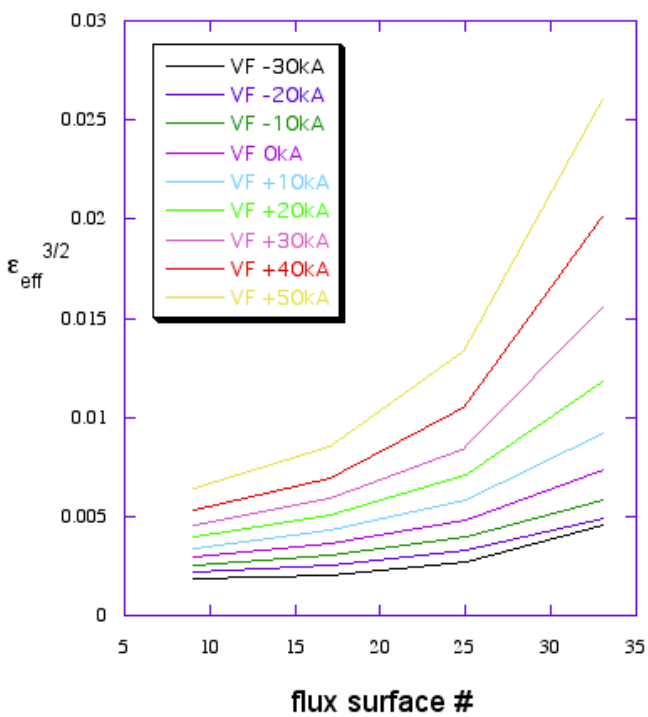

Figure 11 – Variation of $\square_{eff}^{3/2}$ as the vertical field coil currents are changed. I_{VF} = -30 kA corresponds to a shifted-in configuration while I_{VF} = +50 kA corresponds to a shifted-out configuration.

In Figure 12 we plot a similar study as the current in the toroidal field coil current is varied. $\varepsilon_{eff}^{3/2}$ shows less sensitivity to the toroidal field variation than it does to the vertical field variation.

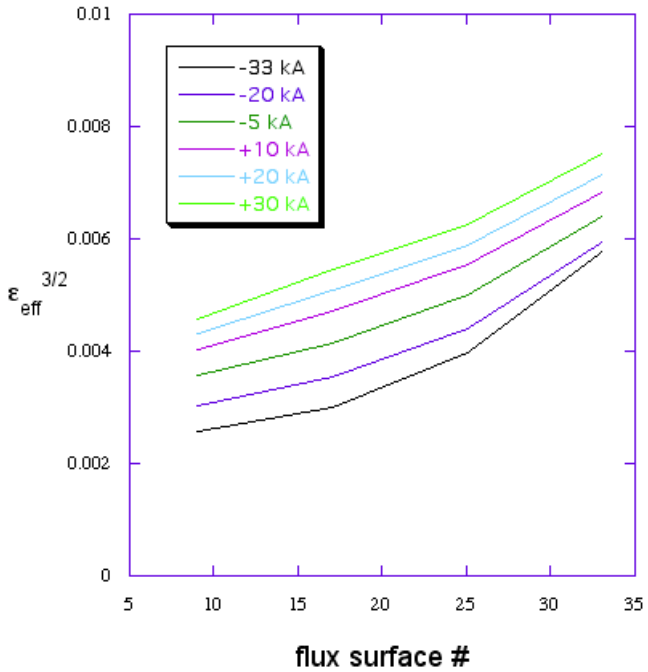

Figure 12 – Variation of $\varepsilon_{eff}^{3/2}$ as the toroidal field coil currents are changed. This is the current level divided over the 12 toroidal coils.

V. Conclusions

Quasi-poloidal symmetry is a new approach to stellarator confinement optimization that has been used to design very low plasma aspect ratio configurations (<R>/<a>≈0.6, 1/2–1/4 that of existing stellarators). This form of symmetry offers reduced flow damping of poloidal flows, reduction of bootstrap current levels by up to a factor of ι/N_{fp} and good neoclassical confinement. We have verified the degree of neoclassical confinement using a variety of analysis tools, including direct measures of the degree of symmetry, the DKES transport coefficient code, the NEO effective ripple code and Monte Carlo global confinement time calculations. Besides verifying that basic configurations can be designed with adequate confinement, we have also found that they possess flexibility through variations of the vertical and toroidal field coil currents for testing a range of confinement issues.

Acknowledgements: This work was supported by U.S. Department of Energy under Contract DE-AC05-00OR22725 with UT–Battelle, LLC.

[1] Boozer, A. H., Phys. Fluids **24,** 1999 (1981).
[2] U. Stroth, et al., Nuclear Fusion **36**, 1063 (1996).
[3] D. A. Spong, S. P. Hirshman, et al., Nuclear Fusion **41**, 711 (2001).
[4] A. Ware, et al., submitted to Phys. Rev. Lett. (2002).
[5] Nemov, V. V., et al., Phys. Plasmas **6**, 4622 (1999).
[6] W. I. Van Rij, S. P. Hirshman, Phys. Fluids B, **1** (March, 1989).
[7] see Chapter 6, section 6.2.3 of "QPS: A Low-Aspect Ratio Quasi-Poloidal Concept Exploration Experment," issued by Oak Ridge National Laboratory in June, 2001 at http://qps.fed.ornl.gov/pvr/docment.htm.